

QR-MIX: Distributional Value Function Factorisation for Cooperative Multi-Agent Reinforcement Learning

Jian Hu

Graduate Institute of Networking and Multimedia
National Taiwan University
r08944053@csie.ntu.edu.tw

Haibin Wu

Graduate Institute of Communication Engineering
National Taiwan University
f07921092@ntu.edu.tw

Seth Austin Harding

Department of Computer Science and Information
Engineering
National Taiwan University
b06902101@csie.ntu.edu.tw

Shih-wei Liao

Department of Computer Science and Information
Engineering
National Taiwan University
liao@csie.ntu.edu.tw

ABSTRACT

In Cooperative Multi-Agent Reinforcement Learning (MARL) and under the setting of Centralized Training with Decentralized Execution (CTDE), agents observe and interact with their environment locally and independently. With local observation and random sampling, the randomness in rewards and observations leads to randomness in long-term returns. Existing methods such as Value Decomposition Network (VDN) and QMIX estimate the mean value of long-term returns while ignoring randomness. Our proposed model QR-MIX introduces quantile regression, modeling joint state-action values as a distribution, combining QMIX with Implicit Quantile Network (IQN). In addition, because the monotonicity in QMIX limits the expression of joint state-action value distribution and may lead to incorrect estimation results in nonmonotonic cases, we design a flexible loss function to replace the absolute weights found in QMIX. Our methods enhance the expressiveness of our mixing network and are more tolerant of randomness and nonmonotonicity. The experiments demonstrate that QR-MIX outperforms prior works in the StarCraft Multi-Agent Challenge (SMAC) environment.

KEYWORDS

Quantile Regression, Randomness, Collaboration, Multi-agent, Reinforcement Learning

ACM Reference Format:

Jian Hu, Seth Austin Harding, Haibin Wu, and Shih-wei Liao. 2021. QR-MIX: Distributional Value Function Factorisation for Cooperative Multi-Agent Reinforcement Learning. In *Proc. of the 20th International Conference on Autonomous Agents and Multiagent Systems (AAMAS 2021), London, UK, May 3–7, 2021*, IFAAMAS, 9 pages.

1 INTRODUCTION

The objective of reinforcement learning (RL) is to maximize the cumulative return of a policy in a given environment. Recent studies such as DQN [16] and AlphaGo [22] demonstrate the remarkable performance of Reinforcement Learning (RL) in game scenarios.

Proc. of the 20th International Conference on Autonomous Agents and Multiagent Systems (AAMAS 2021), U. Endriss, A. Nowé, F. Dignum, A. Lomuscio (eds.), May 3–7, 2021, London, UK. © 2021 International Foundation for Autonomous Agents and Multiagent Systems (www.ifaamas.org). All rights reserved.

However, in some complex scenarios, such as in the collaboration of autonomous vehicles [2] and robot swarms [13], RL remains inapplicable. These scenarios are usually modeled as multi-agent cooperation problems. A natural solution for implementing multi-agent cooperation is Centralized Training with Decentralized Execution (CTDE) in which each agent can make decisions based on its own local observations; in the training phase, data is collected from each agent in addition to global data to increase learning efficiency.

In the multi-agent cooperative task, state-of-the-art methods learn the policy of each agent by decomposing the joint value function. For example, in the discrete action space scenario, VDN [24], QMIX [19], Qatten [27] and other methods achieve excellent results in the SMAC testing environment. In the continuous action space scenario, FacMADDPG [7] proposed by Christian A. Schroeder de Witt et al. extends QMIX functionality to support continuous actions, successfully achieving state-of-the-art performance. Actor-Critic-based methods such as COMA [8] and MADDPG [7] perform relatively poorly in comparison with value-based methods.

However, in MARL, the observation of each agent is local; this typically causes bias and uncertainty in its value function. In addition, random sampling of non-deterministic environments results in randomness [6] in state transitions and rewards obtained. QMIX and VDN ignore randomness and model the mean value of the joint state-action value. To resolve these issues, in the single-agent scenario, Will Dabney et al. collectively proposed C51 [1], QR-DQN [6], and IQN [5] which model the value function as a distribution.

In a recent study, Felipe Leno Da Silva et al. [21] have applied Distributional Independent Q-Learning (C51) to multi-agent Robot Soccer Simulation, achieving better results than Independent Q-Learning (IQL) [26]. However, C51 cannot decompose the joint value, leading to poor results in complex multi-agent cooperation scenarios. Therefore, it proves effective to combine joint value decomposition in unison with Distributional RL [1]. However, with this comes a new set of problems. Studies such as QTRAN [23] have shown that the monotonicity in VDN and QMIX can lead to erroneous value estimation in nonmonotonic cases [15] and also imposes limits on the expressiveness of the joint state-action value distribution. Therefore, we eliminate the hypernet [9] constraint of generating absolute weights in QMIX, and we use the gradient of expectation of the joint state-action value distribution to each

agent’s state-action value as the loss function to decompose the joint state-action value. In comparison with QMIX, this loss imposes fewer constraints on network expressiveness.

Contribution

- (1) We propose Quantile Regression Mixer (QR-MIX) which uses Distributional RL to enhance the tolerance of the model for randomness.
- (2) We design a flexible loss function to replace the absolute weight inherent in QMIX, allowing for higher tolerance of nonmonotonicity and fewer constraints on neural network expressiveness.
- (3) Our experiments demonstrate that QR-MIX outperforms prior works in the SMAC environment [20].

2 BACKGROUND

2.1 Dec-POMDP

A fully cooperative multi-agent task may be described as a decentralized partially observable Markov decision process (Dec-POMDP) composed of a tuple $G = \langle \mathcal{S}, \mathcal{U}, P, r, \mathcal{Z}, O, N, \gamma \rangle$. $s \in \mathcal{S}$ describes the true state of the environment. At each time step, each agent $i \in \mathcal{N} := \{1, \dots, N\}$ chooses an action $u_i \in \mathcal{U}$, forming a joint action $\mathbf{u} \in \mathcal{U} \equiv \mathcal{U}^N$. All state transition dynamics are defined by Function $P(s' | s, \mathbf{u}) : \mathcal{S} \times \mathcal{U}^N \times \mathcal{S} \mapsto [0, 1]$. Each agent has independent observation $z \in \mathcal{Z}$, determined by observation function $O(s, i) : \mathcal{S} \times \mathcal{N} \mapsto \mathcal{Z}$. Variable τ represents agent action-observation history. All agents share the same reward function $r(s, \vec{u}) : \mathcal{S} \times \mathcal{U}^N \rightarrow \mathbb{R}$ and $\gamma \in [0, 1]$ is the discount factor. Given that π^i is the policy of each agent, the objective of the joint agent is to maximize:

$$J(\pi) = \mathbb{E}_{u^1 \sim \pi^1, \dots, u^N \sim \pi^N, s \sim T} \left[\sum_{t=0}^{\infty} \gamma^t r_t(s_t, u_t^1, \dots, u_t^N) \right] \quad (1)$$

2.2 CTDE

Under the Centralized Training with Decentralized Execution (CTDE) framework, the training algorithm has access to all local action-observation history τ and global states, but the learned policy of each agent can condition only on its own action-observation history τ_a . CTDE allows agents to learn and construct a single state-action value function Q_i so that optimizations made at a single level may optimize the joint state-action value function Q_{tot} .

2.3 IGM

An essential concept of multi-agent value function decomposition methods such as VDN [24] and QMIX [19] is Individual-Global-Max (IGM) [23]; given that $\exists Q^i$, the following conditions hold:

$$\arg \max_{\mathbf{u}} Q_{tot}(\tau, \mathbf{u}) = \begin{pmatrix} \arg \max_{u_1} Q_1(\tau_1, u_1) \\ \vdots \\ \arg \max_{u_N} Q_N(\tau_N, u_N) \end{pmatrix} \quad (2)$$

where Q_{tot} is the joint agent value function, τ is the joint agent action-observation history, and \mathbf{u} is joint agent actions. This condition ensures that the Q_{tot} can be decomposed by Q_i .

QMIX and VDN use different methods to ensure that IGM conditions are met. VDN is realized through additivity as in Equation (3), but QMIX is guaranteed through a monotonic network [19], as shown in Equation (4). In its implementation, QMIX uses a hyper-network to generate absolute weights for modeling the non-linear relationship between Q_i and Q_{tot} .

$$\text{(Additivity)} \quad Q_{tot}(\tau, \mathbf{u}) = \sum_{i=1}^N Q_i(\tau_i, u_i) \quad (3)$$

$$\text{(Monotonicity)} \quad \frac{\partial Q_{tot}(\tau, \mathbf{u})}{\partial Q_i(\tau_i, u_i)} \geq 0, \quad \forall i \in \mathcal{N} \quad (4)$$

2.4 Nonmonotonicity

However, in the case of nonmonotonicity [15], VDN and QMIX cannot learn the real optimal action. A simple example of a non-monotonic Q-function is given by the payoff matrix (from [18]) of the two-player three-action matrix game, as shown in Table 1. QMIX’s approximation (right) results in an incorrect state-action value (Table 2).

Table 1: Payoff matrix Table 2: QMIX’s approximation

8	-12	-12
-12	0	0
-12	0	0

-12	-12	-12
-12	0	0
-12	0	0

2.5 Distributional RL

Rather than using a scalar $Q^\pi(s, a)$ as in DQN, Distributional RL [18] takes into account the randomness of Z^π by studying its distribution. The distributional Bellman operator for policy evaluation is defined as

$$Z^\pi(s, u) \stackrel{D}{=} r(s, u) + \gamma Z^\pi(s', u') \quad (5)$$

where $s' \sim P(\cdot | s, u)$ and $u' \sim \pi(\cdot | s')$, and where $A \stackrel{D}{=} B$ denotes that A and B follow the same distribution. The meanings of $P, r(s, u), \pi$ and γ are consistent with those in Dec-POMDP.

With the scalar setting, a distributional Bellman optimality operator can be defined by

$$\mathcal{T}Z(s, u) ::= r(s, u) + \gamma Z \left(s', \arg \max_{u' \in \mathcal{U}} \mathbb{E}Z(s', u') \right) \quad (6)$$

2.6 p - Wasserstein Metric

Bellemare et al. [18] have shown that the distributional Bellman operator is a contraction in the p -Wasserstein metric. The p -Wasserstein distance is the L_p metric of the inverse cumulative distribution function (CDF). The p -Wasserstein distance for random variables U and V with CDF F_U^{-1} and F_V^{-1} , respectively, is given by

$$W_p(U, V) = \left(\int_0^1 |F_U^{-1}(\omega) - F_V^{-1}(\omega)|^p d\omega \right)^{1/p} \quad (7)$$

2.7 Huber Quantile Regression

QR-DQN [6] and IQN [5] estimate the quantile values for each of N fixed, uniform probabilities; the random return is approximated by a uniform mixture of K Diracs,

$$Z_\theta(s, u) := \frac{1}{K} \sum_{i=1}^K \delta_{\theta_i(s, u)} \quad (8)$$

where each θ_i is assigned a fixed quantile target $\theta_i = F_Z^{-1}(\omega_i)$. QR-DQN uses fixed ω_i , whereas IQN samples $\omega_i \sim U([0, 1])$.

IQN and QR-DQN use Huber Quantile Regression [6] for stochastically adjusting quantile estimates and thereby minimize the Wasserstein distance to a target distribution. Given threshold κ , the regression loss is given by

$$\begin{aligned} \rho_\omega^\kappa(\delta_{ij}) &= |\omega - \mathbb{I}\{\delta_{ij} < 0\}| \frac{\mathcal{L}_\kappa(\delta_{ij})}{\kappa}, \quad \text{with} \\ \mathcal{L}_\kappa(\delta_{ij}) &= \begin{cases} \frac{1}{2} \delta_{ij}^2, & \text{if } |\delta_{ij}| \leq \kappa \\ \kappa \left(|\delta_{ij}| - \frac{1}{2} \kappa \right), & \text{otherwise} \end{cases} \end{aligned} \quad (9)$$

on the pairwise TD-errors [25]

$$\delta_{ij} = r + \gamma \theta_j(s', \pi(s')) - \theta_i(s, u) \quad (10)$$

3 QR-MIX

In this section, we propose a new method called Quantile Regression Mixer (QR-MIX). This method combines IQN [5] and QMIX [19] to model the joint state-action value function as a distribution to improve the tolerance of our model for randomness and non-monotonicity. We discuss the benefits of this in detail in Appendix A.

3.1 Quantile Mixing Network

IQN is a deterministic parametric function trained to reparameterize samples from a base distribution, e.g. $\omega \sim U([0, 1])$, to the respective quantile values of a target distribution. IQN provides an effective way to learn an implicit representation of the state-action value distribution.

In Atari games [16], the image embedding network ψ is usually relatively deep, composed of several layers of convolutional neural networks. Therefore, IQN uses a multiplicative form $\psi \odot \phi(\omega_i)$ to force convolutional features to interact with sample embedding and uses cosine to encode the sample ω ,

$$\begin{aligned} \phi_j(\omega) &:= \text{ReLU} \left(\sum_{i=0}^{n-1} \cos(\pi i \omega) w_{ij} + b_j \right) \\ i &:= 1 \dots N, j := 1 \dots N' \end{aligned} \quad (11)$$

where N is the cosine embedding dimension and N' is the image embedding dimension. IQN then uses the result of $\psi \odot \phi(\omega_i)$ to the predict state-action value quantile for each ω_i .

But in QR-MIX, only one layer of the neural network is used for encoding the global state; we therefore use concatenation to interact with sample embedding, as shown in Figure 1. We also simplify cosine embedding as follows:

$$\phi_i(\omega) := \cos(\pi i \omega), i := 1 \dots N \quad (12)$$

Figure 1 shows our mixing network architecture. We input the historical observations and actions of the agent as well as the global state and $\phi(\omega_i)$ to this network, which outputs a joint action value quantile for each ω_i , and we then approximate the expectation of the joint state-action value distribution as

$$\mathbb{E}Z_{tot}(\tau, \mathbf{u}) := \frac{1}{K} \sum_{i=1}^K Z_{tot}(\tau, \mathbf{u}, \phi(\omega_i)) \quad (13)$$

where K is the number of samples.

3.2 Expected-IGM

DEFINITION 1. Expected-Individual-Global-Max (EIGM). For a joint state-action value distribution function $Z_{tot} : \mathcal{T}^N \times \mathcal{U}^N \mapsto \text{Distribution}$, where $\tau \in \mathcal{T}^N$ is joint action-observation history, we assume that there exist individual state-action value functions $[Q_i : \mathcal{T} \times \mathcal{U} \mapsto \mathbb{R}]_{i=1}^N$, such that the following holds

$$\arg \max_{\mathbf{u}} \mathbb{E}Z_{tot}(\tau, \mathbf{u}) = \begin{pmatrix} \arg \max_{u_1} Q_1(\tau_1, u_1) \\ \vdots \\ \arg \max_{u_N} Q_N(\tau_n, u_N) \end{pmatrix} \quad (14)$$

Then $[Q_i]$ satisfies **EIGM** for Z_{tot} under τ . We can also say that the joint action value distribution can be decomposed by $[Q_i]$.

We define

DEFINITION 2. Expected-Monotonicity

$$\frac{\partial \mathbb{E}Z_{tot}(\tau, \mathbf{u})}{\partial Q_i(\tau_i, u_i)} \geq 0, \quad \forall i \in \mathcal{N} \quad (15)$$

corresponding to QMIX's monotonic constraint.

In order to meet the Expected-Monotonicity (2), we can make weights W_1 and W_2 in Figure 1 positive. This condition will ensure that any sample of the distribution Z_{tot} is decomposable for Q_i . However, this strong constraint limits the expressiveness of the mixing network and may lead to an incorrect estimate of the action value (discussed in Section 2.4). Therefore, we propose a new method that uses the gradient of the $\mathbb{E}Z_{tot}$ to Q_i as the loss function,

$$L_{EM} = \sum_i^N \begin{cases} 0, & \text{if } \frac{\partial \mathbb{E}Z_{tot}}{\partial Q_i} \geq 0 \\ -\frac{\partial \mathbb{E}Z_{tot}}{\partial Q_i}, & \text{if } \frac{\partial \mathbb{E}Z_{tot}}{\partial Q_i} < 0 \end{cases} \quad (16)$$

where N is the number of Q_i and $\mathbb{E}Z_{tot}$ is approximated by Equation(13). This loss is designed to impose a penalty for violation of Expected-Monotonicity.

Our method has fewer restrictions on the expressiveness of the mixing network in comparison with absolute weights, especially when we want to express a distribution instead of a scalar. In addition, we do not need for every quantile to be monotonic to keep the expectations monotonic; this property further enhances the model's tolerance for non-monotonic situations.

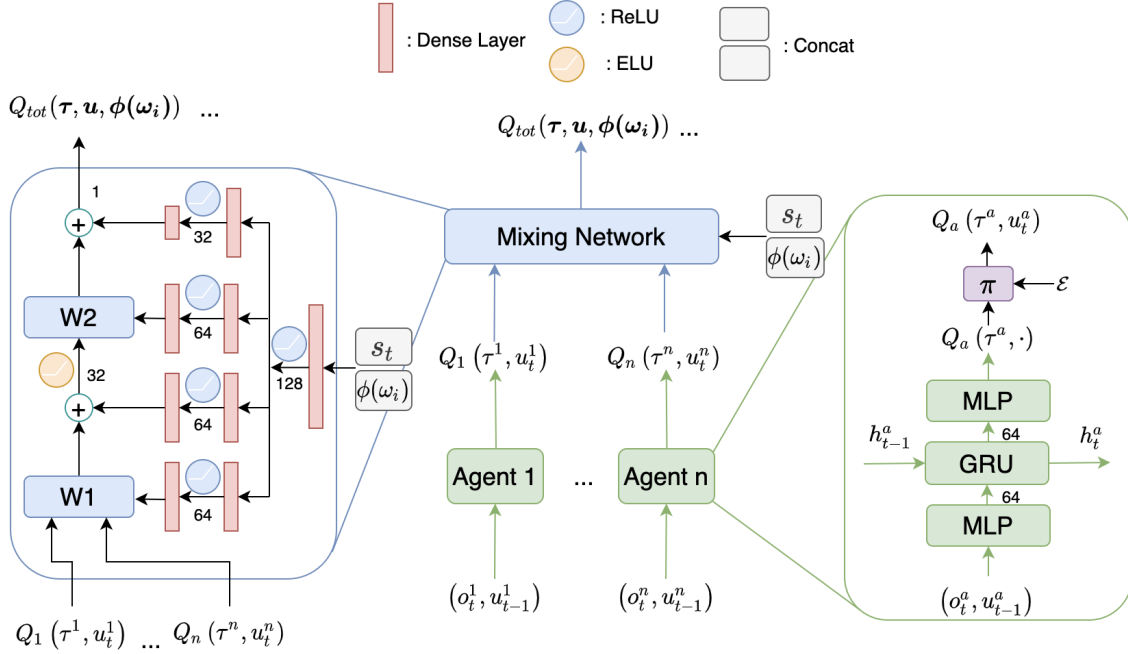


Figure 1: The overall architecture of QR-MIX. On the right is agent i 's recurrent deep Q-network [10], which receives the action-observation history record τ_i (last hidden states h_{t-1}^i , current local observations o_t^i , and last action a_{t-1}^i). On the left is the mixing network of QR-MIX, which mixes $\tilde{Q}^i(\tau_i^i, a_t^i)$ together with s_t and $\phi(\omega_i)$ (Equation 12). $Z_{tot}(\tau, u, \phi(\omega_i))$ is the joint state-action value quantile corresponding to ω_i . The hypernet generates a set of mixing weights for each ω_i .

For calculating the gradient of this loss function, we can use a second-order differential function of the deep learning framework [17].

3.3 Adaptive Loss Function

We use quantile regression in Section 2.7 to train Quantiles Mixing Network, and we add L_{EIGM} (16) and L_{QR} (17) together as L_{TOTAL} (18). In addition, we propose an adaptive coefficient that balances the relationship between the two losses, obviating the issue of the smaller loss may be covered by the larger loss. Given the number of samples K and K' ,

$$\mathcal{L}_{QR} = \frac{1}{K} \sum_{i=0}^{K-1} \sum_{j=0}^{K'-1} \rho_{\omega_i}^K(\delta_{ij}^t) \quad (17)$$

$$\mathcal{L}_{TOTAL} = \mathcal{L}_{QR} + \lambda \cdot \mathcal{L}_{EM} \quad (18)$$

where

$$\lambda = C \cdot \mathcal{L}_{QR} \quad (19)$$

C is a hyperparameter for scaling.

4 EXPERIMENT

4.1 Settings

In this section, we evaluate QR-MIX in StarCraft II decentralized micromanagement tasks and use StarCraft Multi-Agent Challenge (SMAC) environment [20] as our testbed. SMAC consists of a set of StarCraft II micro scenarios used for evaluating how effectively independent agents can learn coordination to solve complex tasks. This environment has become a standard benchmark for evaluating state-of-the-art MARL approaches.

SMAC classifies maps into three difficulty levels: Easy, Hard, and Super Hard. Our test includes maps from each difficulty level. We briefly introduce these maps in Table 5 in Appendix B.

Our main evaluation metric is the relationship between the average winning percentage of the evaluation episodes as a function of environment steps observed over the course of training. This progress can be estimated by periodically running a fixed number of evaluation episodes (actually 32) and disabling any exploratory behavior. We repeat each experiment with many independent training runs, and the results include median performance and percentiles ranging from 25% to 75%. We run the experiment 5 times independently in PyMARL [20]. Each independent run takes between 6 and 13 hours using NVIDIA GeForce GTX 1080Ti graphics cards and Intel(R) Core(TM) i7-7820X CPU.

All hyperparameters in QR-MIX are the same as those found in QMIX [19] and VDN [24] in PyMARL [20] with the exception

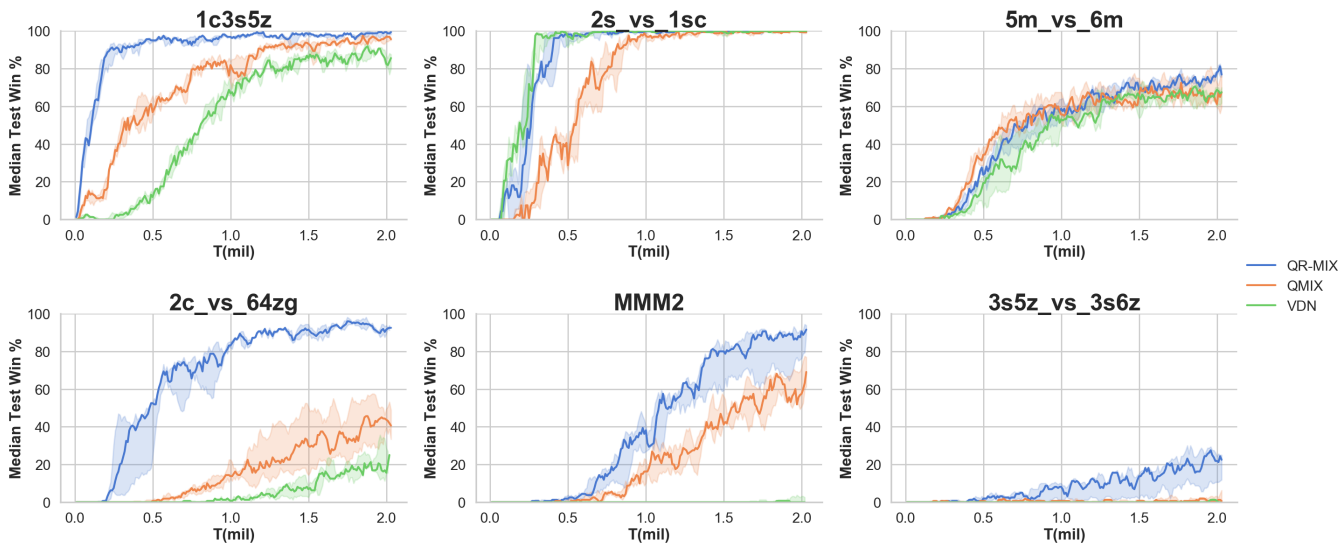


Figure 2: Median win percentage of baselines and QR-MIX. Easy: $2s_vs_1sc$, $1c3s5z$; **Hard:** $5m_vs_6m$, $2c_vs_64_zg$; **Super hard:** $MMM2$, $3s5z_vs_3s6z$.

of hyperparameters used in quantile regression [6], which will be shown in the Appendix B.3.

4.2 Validation

The scenario we tested contains maps of three difficulty levels: Easy, Hard and Super Hard. Easy scenarios include $2s_vs_1sc$, $1c3s5z$, and $2s3z$; Hard scenarios include $5m_vs_6m$, $2c_vs_64_zg$, and $3s_vs_5z$; Super Hard scenarios include $MMM2$ and $3s5z_vs_3s6z$. As shown in Table 5, these maps cover various types, including heterogeneous, homogeneous, micro-trick, etc.

We opt for QMIX and VDN, the best performing model in PyMAREL, as our baseline. We do not use QTRAN as the baseline due to its inferior performance [20] in SMAC. The poor performance of QTRAN may be caused by the fact that in complex scenarios, the approximate loss function does not meet its theoretical conditions. Table 3 shows the final median performance (maximum median across the testing intervals within the last 250,000 steps of training) of the algorithms tested. It can be seen that QR-MIX achieves the best results on all test maps used, especially for Hard and Super Hard maps.

Figure 2 shows the comparison of learning curves between QR-MIX, QMIX, and VDN. It can be seen that except for the two maps $2s_vs_1sc$ and $5m_vs_6m$, the learning speed of QR-MIX is the fastest among all maps. In the Super Hard scenario $3s5z_vs_3s6z$, other methods have not learned effective policies well; however, the median test win rate of QR-MIX slowly improves.

4.3 Ablation Study

In order to analyze the impact of our proposed loss function (16) on performance, we design two comparison methods: (1) **QR-MIX-ABS**, the hypernetwork [9] in QR-MIX-ABS only generates mixing networks with absolute weights; (2) **QR-MIX-FIXED** uses a fixed learning coefficient that sets λ to 1.0.

Table 3: Median performance of the test win percentage in all scenarios

Scenario	QR-MIX	QMIX	VDN
$2s_vs_1sc$	100	100	100
$1c3s5z$	99	97	91
$2s3z$	99	98	97
$5m_vs_6m$	81	69	70
$2c_vs_64zg$	95	45	25
$3s_vs_5z$	98	88	91
$MMM2$	91	69	0
$3s5z_vs_3s6z$	27	1	1

Absolute Weight Figure 3 shows the comparison of the learning curve of QR-MIX, QR-MIX-ABS, and QMIX. In Super Hard scenarios $MMM2$ and $3s5z_vs_3s6z$, QR-MIX performs significantly better than other methods. The positive weight constraint in QR-MIX-ABS limits the expression of joint state-action value distribution in complex scenarios, so it learns more slowly than either QMIX or QR-MIX in $MMM2$. QR-MIX-ABS learning speed is significantly faster than other methods in $3s_vs_5z$, but has a similar learning speed as other algorithms in the final stages of training.

Fixed Coefficient Figure 4 shows the comparison of the learning curve of QR-MIX, QR-MIX-FIXED and QMIX. In Super Hard scenarios $MMM2$ and $3s5z_vs_3s6z$, QR-MIX still performs better than other methods by a large margin. QR-MIX-FIXED performs better than QMIX in $1c3s5z$ and $3s5z_vs_3s6z$. Temporal difference (TD) error [25] in some circumstances may increase with the discovery of new states in MARL. Therefore, if we cannot balance the relationship between $L_{EM}(16)$ and L_{QR} (17), the smaller loss may be covered by the larger loss.

We show the final learning results in Table 4; QR-MIX is shown to have the best average performance, followed by QR-MIX-FIXED.

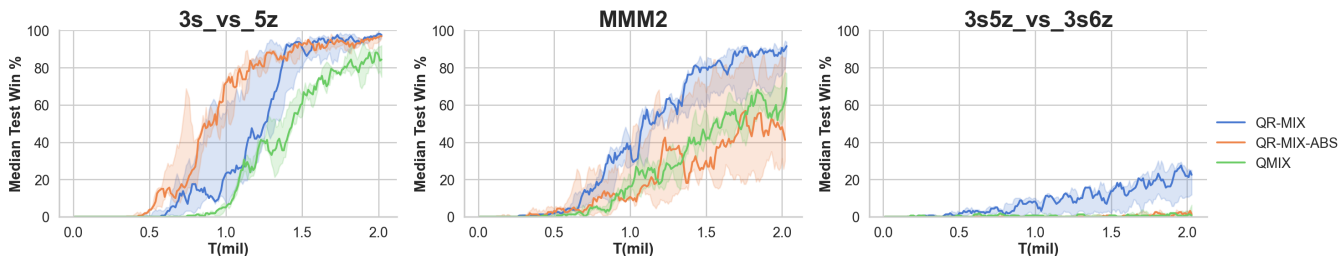


Figure 3: Median win percentage of QR-MIX-ABS. Hard scenarios: 3s_vs_5z; Super Hard scenarios: MMM2, 3s5z_vs_3s6z.

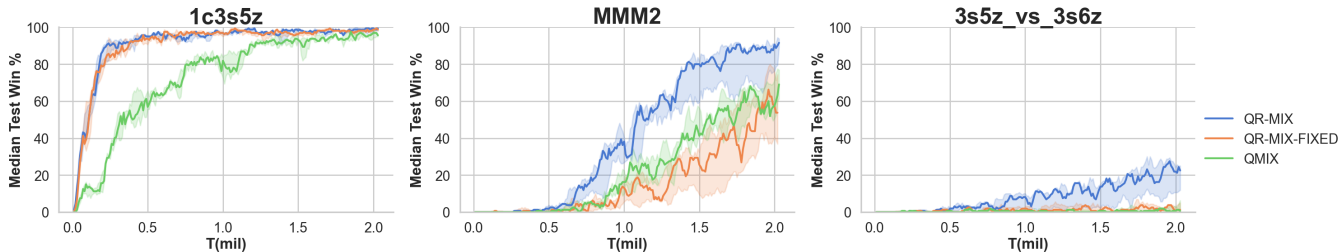


Figure 4: Median win percentage of QR-MIX-FIXED. Easy scenarios: 1c3s5z; Super Hard scenarios: MMM2, 3s5z_vs_3s6z.

Table 4: Median performance of the test win percentage for ablation

Scenario	QR-MIX	QR-MIX-FIXED	QR-MIX-ABS	QMIX
1c3s5z	99	99	99	97
3s_vs_5z	97	96	96	91
MMM2	91	66	55	69
3s5z_vs_3s6z	27	3	3	1

5 CONCLUSION AND FUTURE WORK

In this paper, we propose QR-MIX. We use Distributional RL to enhance the tolerance of our model for randomness. Our proposed loss function contains fewer restrictions on neural network expressiveness and has a higher tolerance for nonmonotonic cases. This enhancement in the expressiveness of the mixing network allows for our method to achieve excellent results. Our method can also be combined with other Mixing Network-based model[27] to improve their ability to express randomness.

However, QR-MIX currently does not consider that the state-action value of each agent also has randomness. Therefore, a more ideal method is to decompose the joint state-action value distribution into the state-action value distribution of each agent. Such modeling will make full use of the benefits of Distributional RL; this is one of our proposed future works.

6 RELATED WORK

Cooperative MARL Both policy-based methods and value-based methods have been proposed for training agents under the CTDE paradigm. Value-based methods are focused on learning a joint state-action value estimator, which may be decomposed into individual state-action value functions such as in VDN [24], QMIX [19], QTRAN [23] and Qatten [27]. Policy-based methods are usually

based on Actor-Critic frameworks such as COMA [8], MADDPG [7], and MAAC [12]. These methods can be applied to continuous action spaces, but they perform poorly in complex scenarios such as SMAC [20]. According to the study by Christian A. Schroeder de Wit and others [7], joint state-action value function decomposition is a key factor in determining the performance of cooperative MARL. They extend QMIX to the continuous action space with Actor-Critic method and achieve state-of-the-art performance. For a complete review of MARL, refer to the survey [11].

Distributional RL DQN [16] models the action-value function as a scalar. However, environments evaluated in RL typically have high randomness; Therefore, Distributional RL considers the factors of randomness, modeling the action-value function as a distribution, and achieves excellent results in Atari games. Will Dabney et al. proposes C51 [1], QR-DQN [6], and IQN [5] successively, perfecting the theory of Distributional RL.

MARL with Distributional RL Felipe Leno Da Silva et al. [21] have applied Distributional Independent Q-Learning (C51) to multi-agent robot soccer simulation, achieving better results than IQL. Xueguang Lyu et al. [14] use IQN to reduce the instability resulting from the exploration behaviors of other agent. However, due to lacking the capability to decompose joint state-action value functions, both C51 and IQN are difficult to apply to complex cooperation scenarios. Our work combines Distributional RL and joint state-action value decomposition, achieving excellent performance.

REFERENCES

- [1] Marc G. Bellemare, Will Dabney, and Rémi Munos. 2017. A Distributional Perspective on Reinforcement Learning. *arXiv:1707.06887 [cs, stat]* (2017).
- [2] Yongcan Cao, Wenwu Yu, Wei Ren, and Guanrong Chen. 2012. An overview of recent progress in the study of distributed multi-agent coordination. *IEEE Transactions on Industrial Informatics* 9, 1 (2012), 427–438.
- [3] Junyoung Chung, Caglar Gulcehre, KyungHyun Cho, and Yoshua Bengio. 2014. Empirical evaluation of gated recurrent neural networks on sequence modeling. *arXiv preprint arXiv:1412.3555* (2014).

- [4] Djork-Arné Clevert, Thomas Unterthiner, and Sepp Hochreiter. 2015. Fast and accurate deep network learning by exponential linear units (elus). *arXiv preprint arXiv:1511.07289* (2015).
- [5] Will Dabney, Georg Ostrovski, David Silver, and Rémi Munos. 2018. Implicit Quantile Networks for Distributional Reinforcement Learning. *arXiv:1806.06923 [cs, stat]* (2018).
- [6] Will Dabney, Mark Rowland, Marc G. Bellemare, and Rémi Munos. 2017. Distributional Reinforcement Learning with Quantile Regression. *arXiv:1710.10044 [cs, stat]* (2017).
- [7] Christian Schroeder de Witt, Bei Peng, Pierre-Alexandre Kamienny, Philip Torr, Wendelin Böhmer, and Shimon Whiteson. 2020. Deep Multi-Agent Reinforcement Learning for Decentralized Continuous Cooperative Control. *arXiv:2003.06709 [cs, stat]* (2020).
- [8] Jakob Foerster, Gregory Farquhar, Triantafyllos Afouras, Nantas Nardelli, and Shimon Whiteson. 2017. Counterfactual Multi-Agent Policy Gradients. *arXiv:1705.08926 [cs]* (2017).
- [9] David Ha, Andrew Dai, and Quoc V Le. 2016. Hypernetworks. *arXiv preprint arXiv:1609.09106* (2016).
- [10] Matthew Hausknecht and Peter Stone. 2017. Deep Recurrent Q-Learning for Partially Observable MDPs. *arXiv:1507.06527 [cs]* (2017).
- [11] Pablo Hernandez-Leal, Bilal Kartal, and Matthew E. Taylor. 2019. A Survey and Critique of Multiagent Deep Reinforcement Learning. *Autonomous Agents and Multi-Agent Systems* 33, 6 (2019), 750–797. <https://doi.org/10.1007/s10458-019-09421-1>
- [12] Shariq Iqbal and Fei Sha. 2019. Actor-Attention-Critic for Multi-Agent Reinforcement Learning. *arXiv:1810.02912 [cs, stat]* (2019).
- [13] Timothy P Lillicrap, Jonathan J Hunt, Alexander Pritzel, Nicolas Heess, Tom Erez, Yuval Tassa, David Silver, and Daan Wierstra. 2015. Continuous control with deep reinforcement learning. *arXiv preprint arXiv:1509.02971* (2015).
- [14] Xueguang Lyu and Christopher Amato. 2020. Likelihood Quantile Networks for Coordinating Multi-Agent Reinforcement Learning. *arXiv:1812.06319 [cs, stat]* (2020).
- [15] Anuj Mahajan, Tabish Rashid, Mikayel Samvelyan, and Shimon Whiteson. 2020. MAVEN: Multi-Agent Variational Exploration. *arXiv:1910.07483 [cs, stat]* (2020).
- [16] Volodymyr Mnih, Koray Kavukcuoglu, David Silver, Alex Graves, Ioannis Antonoglou, Daan Wierstra, and Martin Riedmiller. 2015. Playing Atari with Deep Reinforcement Learning. (2015), 9.
- [17] Adam Paszke, Sam Gross, Francisco Massa, Adam Lerer, James Bradbury, Gregory Chanan, Trevor Killeen, Zeming Lin, Natalia Gimelshein, Luca Antiga, et al. 2019. Pytorch: An imperative style, high-performance deep learning library. In *Advances in neural information processing systems*. 8026–8037.
- [18] Tabish Rashid, Gregory Farquhar, Bei Peng, and Shimon Whiteson. 2020. Weighted QMIX: Expanding Monotonic Value Function Factorisation. *arXiv:2006.10800 [cs, stat]* (2020).
- [19] Tabish Rashid, Mikayel Samvelyan, Christian Schroeder de Witt, Gregory Farquhar, Jakob Foerster, and Shimon Whiteson. 2018. QMIX: Monotonic Value Function Factorisation for Deep Multi-Agent Reinforcement Learning. *arXiv:1803.11485 [cs, stat]* (2018).
- [20] Mikayel Samvelyan, Tabish Rashid, Christian Schroeder de Witt, Gregory Farquhar, Nantas Nardelli, Tim G. J. Rudner, Chia-Man Hung, Philip H. S. Torr, Jakob Foerster, and Shimon Whiteson. 2019. The StarCraft Multi-Agent Challenge. *arXiv:1902.04043 [cs, stat]* (2019).
- [21] Felipe Leno Da Silva, Anna Helena Reali Costa, and Peter Stone. 2019. Distributional Reinforcement Learning Applied to Robot Soccer Simulation. (2019), 5.
- [22] David Silver, Julian Schrittwieser, Karen Simonyan, Ioannis Antonoglou, Aja Huang, Arthur Guez, Thomas Hubert, Lucas Baker, Matthew Lai, Adrian Bolton, et al. 2017. Mastering the game of go without human knowledge. *nature* 550, 7676 (2017), 354–359.
- [23] Kyunghwan Son, Daewoo Kim, Wan Ju Kang, David Earl Hostallero, and Yung Yi. 2019. QTRAN: Learning to Factorize with Transformation for Cooperative Multi-Agent Reinforcement Learning. *arXiv:1905.05408 [cs, stat]* (2019).
- [24] Peter Sunehag, Guy Lever, Audrunas Gruslys, Wojciech Marian Czarnecki, Vinicius Zambaldi, Max Jaderberg, Marc Lanctot, Nicolas Sonnerat, Joel Z. Leibo, Karl Tuyls, and Thore Graepel. 2017. Value-Decomposition Networks For Cooperative Multi-Agent Learning. *arXiv:1706.05296 [cs]* (2017).
- [25] Richard S Sutton and Andrew G Barto. 2018. *Reinforcement learning: An introduction*. MIT press.
- [26] Ardi Tampuu, Tanel Matiisen, Dorian Kodolja, Ilya Kuzovkin, Kristjan Korjus, Juhan Aru, Jaan Aru, and Raul Vicente. 2017. Multiagent cooperation and competition with deep reinforcement learning. *PloS one* 12, 4 (2017), e0172395.
- [27] Yaodong Yang, Jianye Hao, Ben Liao, Kun Shao, Guangyong Chen, Wulong Liu, and Hongyao Tang. 2020. Qatten: A General Framework for Cooperative Multiagent Reinforcement Learning. *arXiv:2002.03939 [cs]* (2020).

Table 5: Part of the Maps in SMAC.

Name	Ally Units	Enemy Units	Type	Difficulty
2s3z	2 Stalkers & 3 Zealots	2 Stalkers & 3 Zealots	heterogeneous & symmetric	Easy
2s_vs_1sc	2 Stalkers	1 Spine Crawler	micro-trick: alternating fire	Easy
1c3s5z	1 Colossi & 3 Stalkers & 5 Zealots	1 Colossi & 3 Stalkers & 5 Zealots	heterogeneous & symmetric	Easy
5m_vs_6m	5 Marines	6 Marines	homogeneous & asymmetric	Hard
2c_vs_64zg	2 Colossi	64 Zerglings	micro-trick: positioning	Hard
3s_vs_5z	3 Stalkers	5 Zealots	micro-trick: kiting	Hard
3s5z_vs_3s6z	3 Stalkers & 5 Zealots	3 Stalkers & 6 Zealots	heterogeneous & asymmetric	Super Hard
MMM2	1 Medivac, 2 Marauders & 7 Marines	1 Medivac, 3 Marauders & 8 Marines	heterogeneous & asymmetric	Super Hard

A WHY LEARN A DISTRIBUTION?

(1) The research of Marc G. Bellemare et al. [1] shows that the Bellman Optimality Operator has a high level of instability in the case of function approximation. (2) Due to local observation and a nondeterministic environment, the same state may correspond to different Q-values. (3) There are more Q-value predictions, some of which may be correct. (4) Only the expectations of the Q-value distribution are guaranteed to remain monotonic; this enhances the tolerance for nonmonotonic cases.

B EXPERIMENTAL SETTINGS

We base our experimental settings on SMAC, which may be referred to in the SMAC paper [20].

B.1 Scenarios

SMAC contains a set of StarCraft 2 micro scenarios designed to evaluate how independent agents may learn to coordinate to solve complex tasks. These scenarios are specially designed to require learning one or more micro-management techniques to defeat the enemy. The scenarios used in our experiment are shown in Table 5.

B.2 PyMAREL

PyMAREL is an open-source framework [20] based on the architecture of SMAC. This framework implements state-of-the-art MARL methods such as COMA, IQL, QMIX, and VDN. We use PyMAREL to conduct a performance comparison.

B.3 Architecture and Hyperparameters

As shown in Figure 1, DRQN is the basic architecture of the agent network [10], containing 64 hidden layer dimensions. A fully connected network layer is put before and after the GRU [3]. The mixing network is a 32-unit single hidden layer network that uses ELU [4] as the activation function. We use a 128-unit fully connected network to mix global state and cosine embedding (12). The mixing results are used in the hyper network to generate mixing network. The hyper network consists of four single hidden layer networks: the dimension of the bottom three hidden layers is 64, and the dimension of the top hidden layer is 32.

We set K and K' equal to 8 to achieve the balance of performance to computational overhead; we set cosine embedding to 32 dimensions, threshold $\kappa = 1$, and coefficient $C = 1$. All agents share a policy network that inputs an ID to distinguish agents. All neural networks are trained using the RMSProp optimizer with

0.0005 learning rates, and we use ϵ -greedy action selection with decreasing ϵ from 1 to 0.05 over 50000-time steps for exploration. For the discount factor, we set $\gamma = 0.99$. The replay buffer size is 5000 episodes and the minibatch size is 32.

C QR-MIX TRAINING ALGORITHM

QR-MIX training algorithms are provided in Algorithm 1.

Algorithm 1: QR-MIX

```
1 Hyperparameters:  $K, K', \kappa, C, \gamma, \epsilon$ 
2 Initialize replay memory  $D$ 
3 Initialize  $[Q_i], Q_{tot}$ , with random parameters  $\theta$ 
4 Initialize target parameters  $\theta^- = \theta$ 
5 for  $episode \leftarrow 1$  to  $M$  do
6   Observe initial state  $\mathbf{s}^0$  and observation  $\mathbf{o}^0 = [O(s^0, i)]_{i=1}^N$  for each agent  $i$ 
7   for  $t \leftarrow 1$  to  $T$  do
8     With probability  $\epsilon$  select a random action  $u_i^t$ 
9     Otherwise  $u_i^t = \arg \max_{u_i^t} Q_i(\tau_i^t, u_i^t)$  for each agent  $i$ 
10    Take action  $\mathbf{u}^t$ , and retrieve next observation and reward  $(\mathbf{o}^{t+1}, r^t)$ 
11    Store transition  $(\tau^t, \mathbf{u}^t, r^t, \tau^{t+1})$  in  $D$ 
12  end
13  Sample a random minibatch of transitions  $(\tau, \mathbf{u}, r, \tau')$  from  $D$ 
14  Sample  $\omega_i, \omega'_j \sim U([0, 1]), \quad 1 \leq i \leq K, 1 \leq j \leq K'$ 
15  Set  $\delta_{ij} \leftarrow r + \gamma Z_{\omega'_j}(\tau', \mathbf{u}^-; \theta^-) - Z_{\omega_i}(\tau, \mathbf{u}; \theta), \quad \forall i, j, \mathbf{u}^- = \left[ \arg \max_{u_i} Q_i(\tau'_i, u_i; \theta^-) \right]_{i=1}^N$ 
16  Calculate  $L_{QR}$  by Equation(17)
17  Calculate  $L_{EM}$  by Equation(16)
18  Calculate adaptive coefficient  $\lambda$  by Equation(19)
19  Update  $\theta$  by minimizing the loss:
    
$$\mathcal{L}_{TOTAL} = \mathbb{E}_{mini\text{-}batch \sim D} (\mathcal{L}_{QR} + \lambda \cdot \mathcal{L}_{EM})$$

20  Update target network parameters  $\theta^- = \theta$  with period  $I$ 
21 end
```
